Lidar-assisted control in wind turbine design: Where are the potential benefits?

H Canet[1], **S Löw**[1], **CL Bottasso**[1]

[1] Wind Energy Institute, Technical University of Munich, Garching, Germany

E-mail: carlo.bottasso@tum.de

Abstract. This study explores the potential benefits of considering Lidar-assisted control (LAC) at the first stages of wind turbine design. The proposed methodology starts with a load analysis of several reference wind turbines to understand which design constraints can be influenced by the use of LAC. The blade and tower of each analyzed model are redesigned considering LAC-induced reductions in key driving quantities. Preliminary results suggest modest reductions in LCOE with potentially significant benefits limited to the tower. The study also discusses the requirements on LAC system purchase and O&M costs, for both onshore and offshore machines, to achieve a reduction in LCOE.

1. Introduction

Turbine-mounted *Light detection and ranging* (Lidar) sensors are able to measure various properties of the incoming wind up to several hundred meters ahead of the wind turbine rotor plane. This preview information has been successfully used to augment conventional feedback controllers with feedforward loops [7], or to replace conventional controllers by advanced predictive ones [13]. These strategies are generically termed *Lidar-assisted control* (LAC).

Multiple studies have concluded that LAC can be used to improve the tracking of C_p, which can lead to an increase of AEP and can reduce fatigue damage and extreme loads in various structural components [7]. These benefits have so far been used to extend the lifetime of existing wind turbines, originally designed to operate with conventional controllers [14].

Even though significant research efforts are currently being devoted to the development of LAC, the benefits of considering LAC within the design of wind turbines are still not fully understood. Within the present work, LAC is considered already at the initial stages of turbine design to fully exploit its potential and reduce Levelized Cost of Energy (LCOE).

This study focuses on two main research questions: first, the paper analyses which key loads can be reduced by a basic LAC implementation and which LCOE reduction can be expected from a LAC-based redesigned turbine. Second, the paper explores the requirements on both the performance and cost of LAC for this device to be economically feasible.

This paper is organized as follows. Sections 2 and 3 are respectively devoted to the description of the approach and the models implemented to answer the two research questions. Section 4 describes the resulting effects of applying LAC at the first stages of design for three different turbines and three different scenarios. Furthermore, the required costs of Lidar are discussed for rendering LAC economically feasible.

2. Approach

The study starts with a load analysis of three reference wind turbines with the goal of understanding the potential reduction margin of their design constraints by the use of LAC. Each model is simulated under a variety of Design Load Cases (DLCs) [12], including power production with normal turbulence (DLC 1.1, DLC 1.2), extreme turbulence (DLC 1.3), loss of electrical network (DLC 2.1) and during extreme operating gusts (DLC 2.3). Also situations where the machine is parked are considered under multiple conditions, such as yaw misalignment (DLC 6.1), grid loss (DLC 6.2) and extreme yaw misalignment (DLC 6.3).

These DLCs are classified into two groups: *modifiable* and *blocking*, according to the influence of the controller on the load envelope. *Modifiable* DLCs are those in which the controller can modify the load envelope. *Blocking* DLCs represent conditions in which the controller performance does not effect the loads, as for example in parked conditions. Table 1 includes a detailed description of the DLCs considered in this study.

The potential load reduction is defined through rankings, where the values of each quantity are ranked in descending order, noting the originating DLC. The value of a key quantity can only be reduced by LAC if the ranking is led by a *modifiable* DLC. Its reduction potential is defined as the difference between its absolute maximum value and the value of the highest ranked *blocking* DLC.

As a second step, a baseline LAC load-reduction model is applied to the resulting loads of all *modifiable* DLCs. This model replaces the simulation of LAC and consists in the application of load-reduction coefficients to the load envelope resulting from aeroelastic simulations with a *non-LAC* controller. Differently performing LAC systems are considered by introducing an optimistic and a pessimistic scenario, defined by a correction factor. This factor multiplies the load-reduction coefficients and is defined as 1.5 for the optimistic scenario, 1 for the baseline scenario and 0.5 for the pessimistic one. The presented method intentionally does not commit to a specific Lidar hardware or controller types, and thus enables a fast preliminary generic assessment for design purposes. Finally, for all three scenarios, the structural redesign of the blades and tower is performed. The resulting changes in the structure are evaluated from an economic point of view through corresponding cost models, according to the wind turbine characteristics.

Table 1: Classification of Design Load Cases (DLC) according to the influence of the controller on the wind turbine load envelope. NTM = Normal Turbulence Model; ETM = Extreme Turbulence Model; EOG = Extreme Operating Gust; EWM = Extreme Wind speed Model

Classification	DLC	Seeds	Design situation	Wind speed	Wind profile	Other condition
Modifiable	1.1	3	Power production	V_{in}:V_{out}	NTM	
	1.2	3	Power production	V_{in}:V_{out}	NTM	
	1.3	3	Power production	V_{in}:V_{out}	ETM	
	2.1	3	Power production	V_{in}:V_{out}	NTM	Grid loss
	2.3 V_o	1	Power production	V_{out}	EOG	Grid loss
	2.3 V_r	1	Power production	$V_{rated} \pm 2m/s$	EOG	Grid loss
Blocking	6.1	3	Parked	V_{ref}	EWM 50 year	Yaw mis. $\pm 8^\circ$
	6.2	3	Parked	V_{ref}	EWM 50 year	Grid loss
	6.3	3	Parked	V_{ref}	EWM 1 year	Ext. yaw mis. $\pm 20^\circ$

3. Methodology and models

3.1. Aeroelastic simulation and design procedure

Aeroelastic calculations are performed with the Blade Element Momentum (BEM) based aeroelastic simulator `Cp-Lambda` (Code for Performance, Loads, Aeroelasticity by Multi Body Dynamic Analysis) [6], coupled with a conventional non-LAC controller [13]. This aeroelastic simulator is also the core of the wind turbine design suite, `Cp-Max` [1]. This code can perform the combined preliminary optimization of a wind turbine, including both blade and tower sizing. The optimization of the blade aeroelastic characteristics can be divided into two smaller sub-loops, which size the external aerodynamic shape and the structural components separately. In this work, the aerodynamic shape is kept frozen, and the turbine is redesigned only from the structural point of view. The structural optimization algorithm aims at minimizing blade cost, while guaranteeing its structural integrity and other requirements by enforcing a set of constaints. The optimization variables include the thickness of the structural elements for given blade layout and materials. The inertial and structural characteristics of each blade section are computed with the 2D finite element cross-sectional analysis code ANBA [10].
The tower structural sizing aims at minimizing tower cost, while satisfying a number of constraints to ensure the safety of the machine and other design requirements. The optimization variables include the diameter and thickness of the different tower segments for given material characteristics. The formal description of these algorithms can be found in [4, 1]. Both the blade and tower procedures employ a Sequential Quadratic Programming (SQP) optimization algorithm, in which gradients are computed by means of forward finite differences.

3.2. Baseline LAC load-reduction model

Multiple studies in the literature report the effects of LAC on loads for different controller formulations, such as feedforward, Linear Quadratic Regulator (LQR) or Model Predictive Control (MPC). Within these references, one specific study [7] is chosen to define the load-reduction model employed here. Reference [7] used a simple feedforward Lidar-assisted controller in combination with a conventional feedback controller on a 5 MW turbine.
The work reports reductions on an extensive set of loads for multiple components such as blade, tower and main bearing. Large reduction of fatigue loads resulting from DLC 1.2 for blade, main bearing, tower top and tower base are observed. Extreme loads resulting from DLC 2.3 also significantly benefit from the implementation of LAC. Table 2 reports the considered reduction coefficients for each component and *modifiable* DLC. For simplicity, this model does not include Lidar faults and assumes a Lidar availability of 100%.
DLC 2.1 deserves a specific discussion. Even though it is in principle a *modifiable* DLC, the precise estimation of LAC-induced reductions of extreme loads is difficult in this case. Extreme loads usually result from the wind turbine shut-down manoeuvre after grid disconnection. Since the wind excitation and the time at which grid loss occurs are both random, the state of the turbine at the time the shut-down manoeuvre is initatied is also random. This clearly makes it difficult to reliably estimate the load reduction, unless as specific dedicated simulation is conducted. Since these LAC-induced load reductions are still not fully described in the literature, they are here considered to be negligible.
In terms of Annual Energy Production (AEP), benefits are assumed to be 0.2% below rated speed and nonexistent above rated speed [7].

3.3. Cost models

The economic assessment is performed with different cost models. The SANDIA Blade Cost Model [11] is used to compute the blade cost for both onshore and offshore models. The 2015 NREL Cost Model [16], an updated version of the 2006 model [9], is applied for onshore machines, while the INNWIND Cost Model [8] is used for the study on offshore machines. The outputs

of both models are expressed in 2020€, correspondingly inflated with the consumer price index and exchange rate. In order to ensure its comparability, LCOE is computed as

$$LCOE = \frac{FCR \cdot ICC}{AEP} + AOE, \tag{1}$$

where FCR [−] is the Fixed Change Rate, assumed to be 7%, ICC [€] is the Initial Capital Cost, AEP [MWh] is the Annual Energy Production and AOE [€/MWh] are the Annual Operating Expenses.
In addition to the standard turbine costs, the costs for the Lidar system have to be considered. Very conservative cost values for purchase and O&M of the Lidar hardware have been considered, based on the information from two major Lidar manufacturers. It has been assumed that two Lidar scanners have to be purchased over a turbine lifetime of 20 years. This results in additional 100,000€ of ICC and 2,500€/year of AOE. Only hardware-related costs have been regarded. Due to lack of information, the costs of development or licensing of Lidar-assisted turbine control software, related commissioning and software maintenance have been neglected.

Table 2: Load reduction coefficients considered in the baseline LAC load-reduction model

BLADE							
	Description	Fx	Fy	Fz	Mx	My	Mz
DLC 1.1 & 1.3	Extreme loads					-2.0%	
	Tip deflection					-2.0%	
DLC 1.2	DEL	-3.8%	-0.1%	-0.25%	-0.4%	-3.8%	-3.5%
DLC 2.3	Extreme loads					-2.9%	
	Tip deflection					-2.9%	
MAIN BEARING							
	Description	Fx	Fy	Fz	Mx	My	Mz
DLC 1.1 & 1.3	Extreme loads						
DLC 1.2	DEL	-10.0%			-1.2%	-0.4%	-1.0%
TOWER TOP (YAW BEARING)							
	Description	Fx	Fy	Fz	Mx	My	Mz
DLC 1.1 & 1.3	Extreme loads						
DLC 1.2	DEL	-12.0%	-0.1%	-2.1%	-2.0%	-1.8%	-0.2%
TOWER BASE							
	Description	Fx	Fy	Fz	Mx	My	Mz
DLC 1.1 & 1.3	Extreme loads					-5.0%	
DLC 1.2	DEL	-3.0%	0.2%	-2.2%	-0.1%	-12.0%	-0.2%
DLC 2.3	Extreme loads					-40.0%	

4. LAC-based effect on LCOE

4.1. Analyzed reference machines

The study is performed on three reference machines of different wind classes: an offshore 10 MW turbine (1A) [6] and two onshore machines: a 2.2 MW (2A) [1] and a 3.4 MW (3A) [2]

turbine. The general characteristics of these turbines, including blade length and tower height, are described in Table 3. A detailed characterization of these machines can be found in the corresponding references.

Table 3: Main characteristics of the reference models included in the study

Turbine	1 [6]	2 [1]	3 [2]
IEC Class & Category	1A	2A	3A
Rated electric power [MW]	10	2.2	3.4
Rotor diameter [m]	178.3	92.4	130.0
Specific power $[W/m^2]$	400.5	298.3	252.4
Hub height [m]	119.0	80.0	110.0
Blade mass [t]	42.5	8.6	16.4
Tower mass [t]	628	125	553

These machines are representative of currently installed wind turbines. The costs of these three machines are compared to the costs of reference projects in the US in terms of capital (CAPEX), operational expenses (OPEX), AEP and LCOE. The first three figures are normalized by rated power. Table 4 shows a good match between the costs of the onshore 2A machine and a generic 2.32 MW turbine of a reference onshore project in the US in 2017 [15]. The costs of the 3A turbine, even if slightly higher for some figures, also follow well the values of the reference turbine. In the second column, the costs of a bottom-fixed offshore 5 MW machine are compared with the 1A machine used in this study. Large differences are found here, for instance in OPEX costs, due to the very different rating of the turbines. In general, the cost distribution presents a similar pattern to the considered reference. The cost breakdown comparison is expressed in 2017 United States Dollars (USD) and CAPEX does not include financial costs. LCOE has been recomputed in all cases as indicated in Eq. (1).

Table 4: Comparison of cost breakdown of the different reference models in 2017 USD

	Onshore			Offshore	
	Stehly et al. [15]	2A	3A	Stehly et al. [15]	1A
Rating [MW]	2.32	2.2	3.4	5	10
CAPEX [USD/kW]	1454	1297	1759	3846	4379
OPEX [USD/kW]	43.6	48.1	51.4	144	225
AEP [MWh/MW]	3633	3520	3866	3741	4500
FCR [%]	7.9	7.9	7.9	7.0	7.0
LCOE [USD/MWh]	43.6	42.9	49.2	110.5	118.1

4.2. Load analysis: Potential reduction margins

The analysis of the load rankings highlights important potential reduction margins that could be exploited by LAC. Figure 1 provides an overview of the ranking position of the first *blocking* DLC for each machine.

Blade tip deflection: As shown in Fig. 1a, this ranking is led by *modifiable* DLCs and reductions are blocked by DLC 2.1 for all machines. More specifically, the reduction margin for turbine 1A is blocked at ranking position 7, for turbine 3A at ranking position 20, and for turbine 2A at ranking position 28. The analysis unveils potential reduction margins of tip displacement between 8% (1A) and 21% (2A). These margins could be exploited in the design of the blade, since maximum tip deflection is typically an important active design driver for the spar caps.

Extreme loads: The analysis of the combined blade root moment ranking (Fig. 1b) leads to similar conclusions. Indeed, DLC 2.1 is here also the first *blocking* DLC to appear for the three turbines, with large potential reduction margins in machines 2A and 3A.
Combined bending moment at tower top (Fig. 1c) shows no potential margin for machine 1A, and reduced margins for turbines 2A and 3A. This potential reduction could relax the buckling constraint. No potential reduction margin is found at tower bottom (Fig. 1d), a load clearly driven by *blocking* cases.

Fatigue: In the case of fatigue, only DLC 1.2 has to be considered according to the standards. Thus, there are no *blocking* DLCs and fatigue reductions from LAC fully translate into relaxed design constraints.

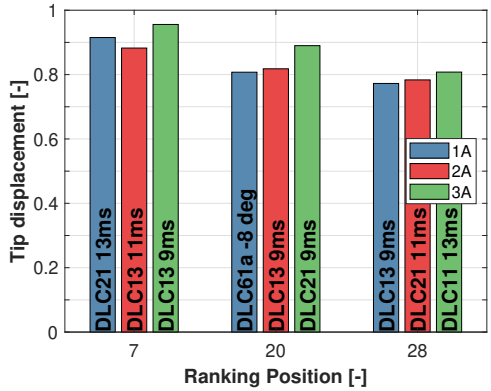

(a) Blade tip deflection

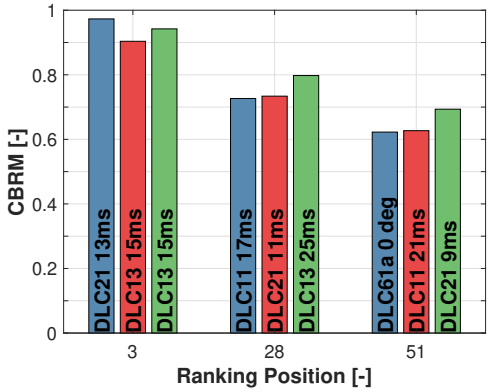

(b) Combined blade root moment (CBRM)

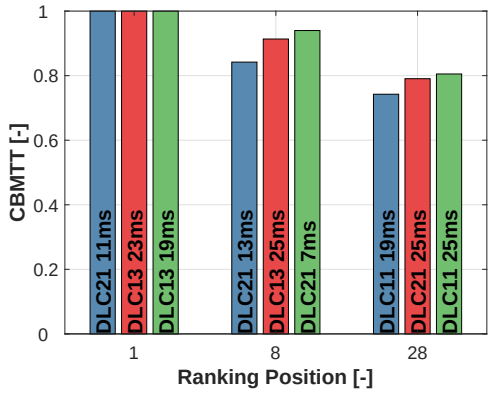

(c) Combined bending moment at tower top (CBMTT)

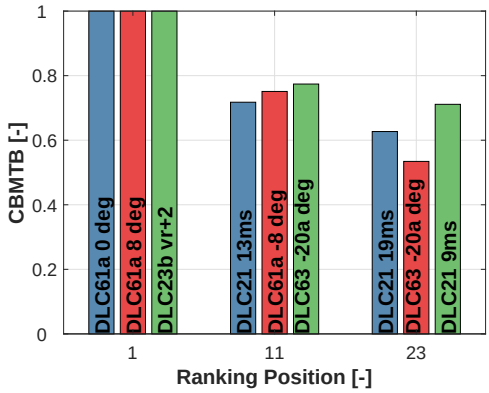

(d) Combined bending moment at tower bottom (CBMTB)

Figure 1: Ranking position of the first appearing *blocking* case for different key quantities and machines. Results are normalized with the maximum load of the respective turbine.

4.3. LAC-induced reductions in blade and tower mass

For the LAC-based redesign of the turbines, the load-reduction coefficients of Table 2 are applied to the loads resulting from initial *non-LAC* runs of all DLCs. Consequently, the design parameters are varied until convergence of the SQP algorithm. This sequence of simulation, application of reduction margins and optimization is repeated until convergence.

The LAC-based redesign leads to large reductions in tower mass and more modest savings in blade mass, as reported in Fig. 2.

Tower: Both the 1A and 3A towers enjoy significant benefits from the large reductions in fatigue and achieve a mass reduction between approximately 17% for the optimistic scenario and approximately 5% for the pessimistic one.

The tower of the 2A machine presents a smaller improvement due to different active design drivers. Indeed, this model presents an increased importance of the buckling constraints when compared to the other turbines. Even though a potential reduction margin of 10% was found in the load analysis for combined bending moment at tower top (Fig. 1c) —a load that may drive the tower buckling behavior— this is not reduced by LAC according to the applied load-reduction model (Table 2), and therefore cannot be exploited.

Blades: Modest reductions are achieved at the blades of all models and for all scenarios, due to the moderate influence of LAC in design-driving constraints. Even though a large potential margin was found for tip deflection, the applied LAC load-reduction model in Table 2 only allows for a reduction of 2%.

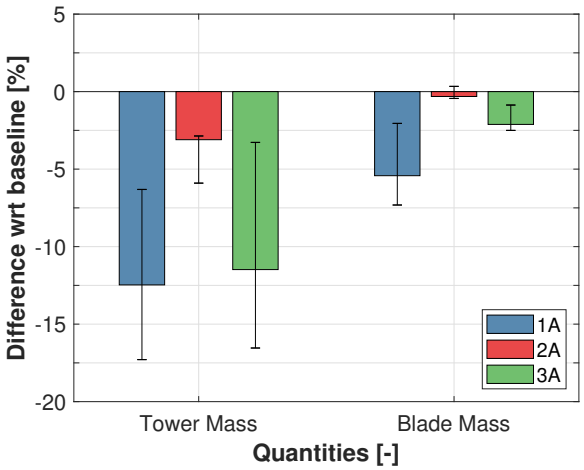

Figure 2: LAC-induced reductions in tower mass and blade mass. The confidence intervals show the values for the optimistic (lower end) and pessimistic scenarios (upper end), introduced by a correction factor.

4.4. LAC-induced reductions in LCOE

LAC-generated improvements not always translate into noticeable LCOE changes. For the 2A turbine, low tower mass reductions in combination with the significant Lidar costs clearly lead to an increase of LCOE. More interesting conclusions are obtained when analyzing the 1A and 3A machines.

While both machines present significant reductions in ICC, a different effect is observed in annual operating expenses (AOE). Indeed, the additional expenses created by maintenance of the Lidar system do not significantly increase the overall AOE for offshore machines, due to the already high O&M expenses. For onshore machines, these costs play a larger role and increase AOE by approximately 2%.the Additionally, AEP is slightly increased for both onshore and offshore

machines. While turbine 1A achieves reductions between 0.5% and 2% in LCOE, for machine 3A a slight decrease of 0.5% is achieved with the best performing scenario.
The reduction in ICC reached by the blade redesign is generally not high enough to compensate for the increase of AOE. Therefore LCOE increases for all onshore machines and slightly decreases for the offshore machine.

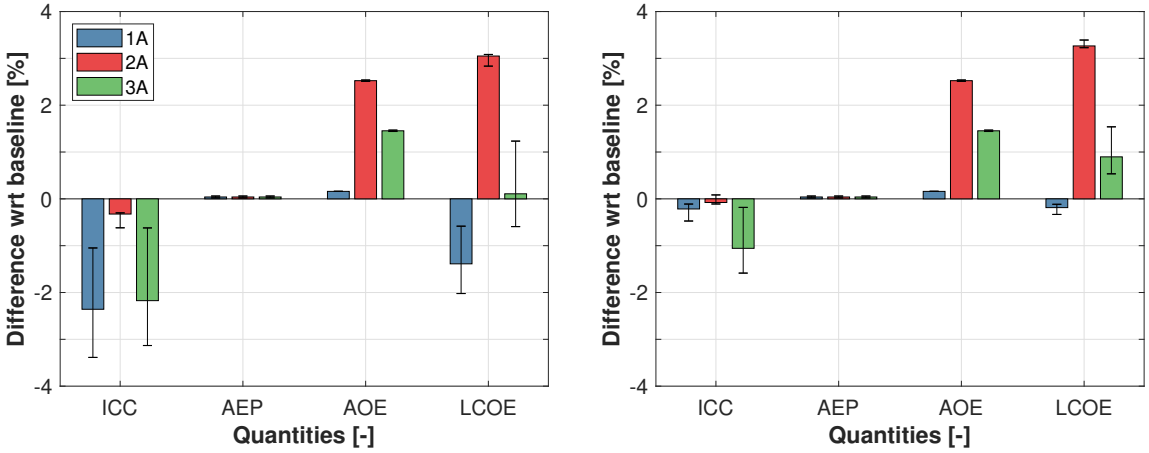

(a) LAC-induced redesigned tower (b) LAC-induced redesigned blade

Figure 3: LAC-induced reductions in Initial Capital Costs (ICC), Annual Energy Production (AEP), Annual Operating Expenses (AOE) and Levelized Cost Of Energy (LCOE) for tower (left) and blade redesigns (right). The confidence intervals show the values for the optimistic (lower end) and pessimistic scenarios (upper end), introduced by the correction factor.

4.5. Cost sensitivity analysis

Finally, a cost sensitivity analysis is performed to understand how the purchase and maintenance cost of a Lidar system can influence the reduction in LCOE. The analysis is performed on the scenario with baseline LAC load-reduction coefficients.
In the case of the 1A machine (Fig. 4a), LCOE shows little variability when both purchase and maintenance costs are modified. Larger effects are observed for the 3A machine (Fig. 4b). Here an increase or redution of LCOE can be obtained by modifying the LAC system costs. Both machines show modest reductions in LCOE, even with very low LAC costs, implying that a real effect on LCOE can only be achieved by an improved LAC performance in some key loads.

5. Conclusions

This paper has presented a preliminary analysis on the potential benefits of considering LAC at the first stages of wind turbine design. A first load analysis highlights an interesting potential for the blade as well as for fatigue-driven tower designs. For instance, potential reduction margins of up to 20% are observed in tip deflection, as well as in the combined bending moment at tower top. The current LAC systems are only partially exploiting the reduction potential of these loads. Indeed, according to the load-reduction model considered here, blade tip deflection is reduced up to 2% and combined bending moment at tower top is not reduced, leading to negligible benefits for the rotor and buckling-driven towers. Fatigue-driven towers enjoy a more significant effect, since fatigue is greatly reduced by LAC.
In terms of LCOE, the offshore machine shows the largest reductions for all considered systems. This turbine significally benefits from the reduced influence of the additional LAC-based costs, given the already high O&M and ICC figures. In this case, the purchase and O&M costs of

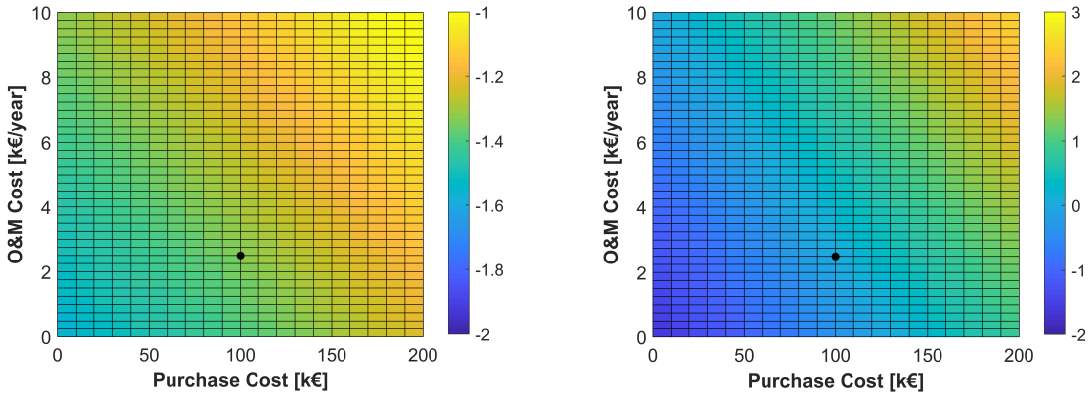

(a) Machine 1A (b) Machine 3A

Figure 4: Sensitivity analysis of the effect of the purchase and O&M cost of LAC systems on LCOE reduction for the offshore (1A) and onshore (3A) machines. The baseline costs are indicated with a black circle.

Lidar do not play a large role in the overall achieved LCOE reduction. For the onshore machine, the effect on LCOE shows a higher sensitivity to the performance and costs of a LAC system.

This study only partially explores the benefits of introducing LAC in the early stages of wind turbine design. Indeed, even though this study gave some insight into how design differences in the tower can influence the LAC-induced benefits, a deeper analysis of the design drivers should be performed to get a more complete picture. Additionally, the list of analyzed DLCs should be expanded to include other design conditions that occasionally result in design drivers, such as DLC 1.4 (power production with extreme coherent gust with direction change) or DLC 1.5 (power production with extreme wind shear). Further work should also analyze the effects of a reduced Lidar availability, since the current load-reduction model assumes an availability of 100%. Additionally, other applications of LAC should be explored. For instance, LAC-induced lower loading could be exploited to increase hub height and gain power capture. Finally, it should be remarked that the use of a generic load model implies some significant approximations, and more precise conclusions could be obtained with the use of a Lidar simulator and a specific controller implementation.

6. Acknowledgements

The authors would like to thank the participants of the IEA Task 32+37 workshop “Optimizing Wind Turbines with Lidar-Assisted Control using Systems Engineering” for the valuable discussions.

7. References

[1] Bortolotti P and Bottasso CL and Croce A 2016 Combined preliminary-detailed design of wind turbines *Wind Energ. Sci.* **1** 71-88 10.5194/wes-1-71-2016

[2] Bortolotti P, Canet H, Dykes K, Merz K, Sethuraman L, Verelst D and Zahle F 2019 IEA Wind TCP Task 37: Systems engineering in wind energy - WP2.1 Reference wind turbines *National Renewable Energy Laboratory technical report* Golden, CO 10.2172/1529216

[3] Bottasso CL, Croce A, Savini B, Sirchi W and Trainelli L 2006 Aero-servo-elastic modeling and control of wind turbines using finite-element multibody procedures. *Multibody Syst. Dyn.* **16** 291-308 10.1007/s11044-006-9027-1

[4] Bottasso CL, Campagnolo F and Croce A 2012 Multi-disciplinary constrained optimization of wind turbines *Multibody Syst. Dyn.* **27** 21-53 10.1007/s11044-011-9271-x

[5] Bottasso CL, Croce A, Nam Y and Riboldi CED 2012 Power curve tracking in the presence of a tip speed constraint *Ren. En.* **40** 1-12 10.1016/j.renene.2011.07.045
[6] Bottasso CL, Bortolotti P, Croce A and Gualdoni F 2016 Integrated aero-structural optimization of wind turbines *Multibody Syst. Dyn.* **38** 317-344 10.1007/s11044-015-9488-1
[7] Bossanyi E, Kumar A and Hugues-Salas O 2014 Wind turbine control applications of turbine-mounted Lidar *J. Phys.: Conf. Ser.* **555** 012011 10.1088/1742-6596/555/1/012011
[8] Chaviaropoulos P, Karga I, Harkness C and Hendriks B 2014 Deliverable 1.23 PI-Based assessment of innovative concepts *INNWIND.EU technical report*
[9] Fingersh L, Hand M and Laxson A 2006 Wind turbine design cost and scaling model *National Renewable Energy Laboratory technical report* Golden, CO NREL/TP-500-40566
[10] Giavotto V, Borri M, Mantegazza P and Ghiringhelli G 1983 Anisotropic beam theory and applications *Comput. Struct.* **16** 403-13 10.1016/0045-7949(83)90179-7
[11] Griffith DT and Johans W 2013 Large blade manufacturing cost studies using the sandia blade manufacturing cost tool and Sandia 100-meter blades *Sandia National Laboratories technical report* Albuquerque, NM SAND2013-2734
[12] International Electrotechnical Commission 2005 IEC 61400-1 Ed.3: Wind turbines - Part 1: Design requirements
[13] Riboldi CED 2012 Advanced control laws for variable-speed wind turbines and supporting enabling technologies *Politecnico di Milano Doctoral dissertation* Milan, Italy
[14] Schlipf D, Fürst H, Raach S and Haizmann F 2018 Systems engineering for Lidar-assisted control: A sequential approach. *J. Phys.: Conf. Ser.* **1102** 012014 10.1088/1742-6596/1102/1/012014
[15] Stehly T, Beiter P, Heimiller D and Scott G 2017 Cost of wind energy review *National Renewable Energy Laboratory technical report* Golden, CO NREL/TP-6A20-72167
[16] WISDEM Repository 2020 github.com/WISDEM